nature cities

Article

https://doi.org/10.1038/s44284-025-00227-9

A strong but uneven increase in urban tree cover in China over the recent decade

Received: 28 June 2023

Accepted: 12 March 2025

Published online: 22 April 2025

Check for updates

Xiaoxin Zhang[1,2] ✉, Martin Brandt[1] ✉, Xiaoye Tong[1], Xiaowei Tong[3,4], Wenmin Zhang[1], Florian Reiner[1], Sizhuo Li[1], Feng Tian[5], Yuemin Yue[3,4], Weiqi Zhou[6], Bin Chen[2,7], Xiangming Xiao[8] & Rasmus Fensholt[1]

Trees play a crucial role in urban environments, offering various ecosystem services that contribute to public health and human well-being. China has initiated a range of urban greening policies to increase the number of urban trees, but monitoring urban tree dynamics at a national scale has proven challenging. Here, we used high-resolution nanosatellite images to quantify urban tree cover in all major Chinese cities in 2019 and study changes in tree cover between 2010 and 2019. We show that 11.47% of urban areas were covered by trees in 2019, and 76% of the cities experienced an increase in tree cover compared with 2010. Notably, the increase in tree cover in the mega-cities of Shanghai, Beijing, Shenzhen and Guangzhou (6.64%) was higher than that in other cities analyzed. Tree cover increases also vary between urban land use types, with public service (3.09%) and residential areas (1.79%) having the highest values. The study employed a data-driven approach toward assessing urban tree cover changes, showing clear signs of overall increases that nonetheless do not benefit all cities equally.

China's rapid urbanization during the past two decades has led to the creation of millions of new houses and extensive impervious surfaces, often at the expense of agricultural land and forests[1,2]. Mega-cities are often associated with diminished quality of life due to pervasive environmental issues such as traffic congestion, air pollution and the dominance of concrete landscapes[3]. To enhance the well-being and living conditions of residents in Chinese cities, urban greening policies have been implemented since 1992 and have been further promoted since 2000[4,5]. For example, the 'Ordinance for Urban Greening' program provides guidance on planning and establishing green spaces in built-up areas[4]. Additionally, the 'National Forest City' program, launched in 2004, emphasizes the promotion of urban forests as nature-based solutions to contribute to achieving a sustainable urban environment[5]. These policies have prioritized the establishment of green spaces and urban parks around public and residential areas, the plantation of trees along roads and the construction of urban ecological corridors[4,6]. Trees are a major component of greening policies and play a vital role in urban environments, being placed in parks, yards, gardens and along streets, thus serving as an essential element of urban life[7,8]. Large urban trees offer a range of ecological and socioeconomic benefits, such as the mitigation of urban heat islands[9,10], reduced energy consumption[11], increased carbon sequestration[12], air purification[13], reduced water runoff[14], shade[15] and biodiversity[16], consequently improving human well-being and health[12]. Several studies have documented that urban trees provide benefits for municipalities and their residents, and local, regional and global initiatives have promoted the planting and

[1]Department of Geosciences and Natural Resource Management, University of Copenhagen, Copenhagen, Denmark. [2]Future Urbanity and Sustainable Environment (FUSE) Lab, Division of Landscape Architecture, Faculty of Architecture, The University of Hong Kong, Hong Kong, China. [3]Institute of Subtropical Agriculture, Chinese Academy of Sciences, Changsha, China. [4]Guangxi Key Laboratory of Karst Ecological Processes and Services, Huanjiang Observation and Research Station of Karst Ecosystem, Chinese Academy of Sciences, Huanjiang, China. [5]Hubei Key Laboratory of Quantitative Remote Sensing of Land and Atmosphere, School of Remote Sensing and Information Engineering, Wuhan University, Wuhan, China. [6]State Key Laboratory for Ecological Security of Regions and Cities, Research Center for Eco-Environmental Sciences, Chinese Academy of Sciences, Beijing, China. [7]Institute for Climate and Carbon Neutrality, Urban Systems Institute, The University of Hong Kong, Hong Kong, China. [8]School of Biological Science, Center for Earth Observation and Modeling, University of Oklahoma, Norman, OK, USA. ✉e-mail: xzh@ign.ku.dk; mabr@ign.ku.dk

https://doi.org/10.1038/s44284-025-00227-9

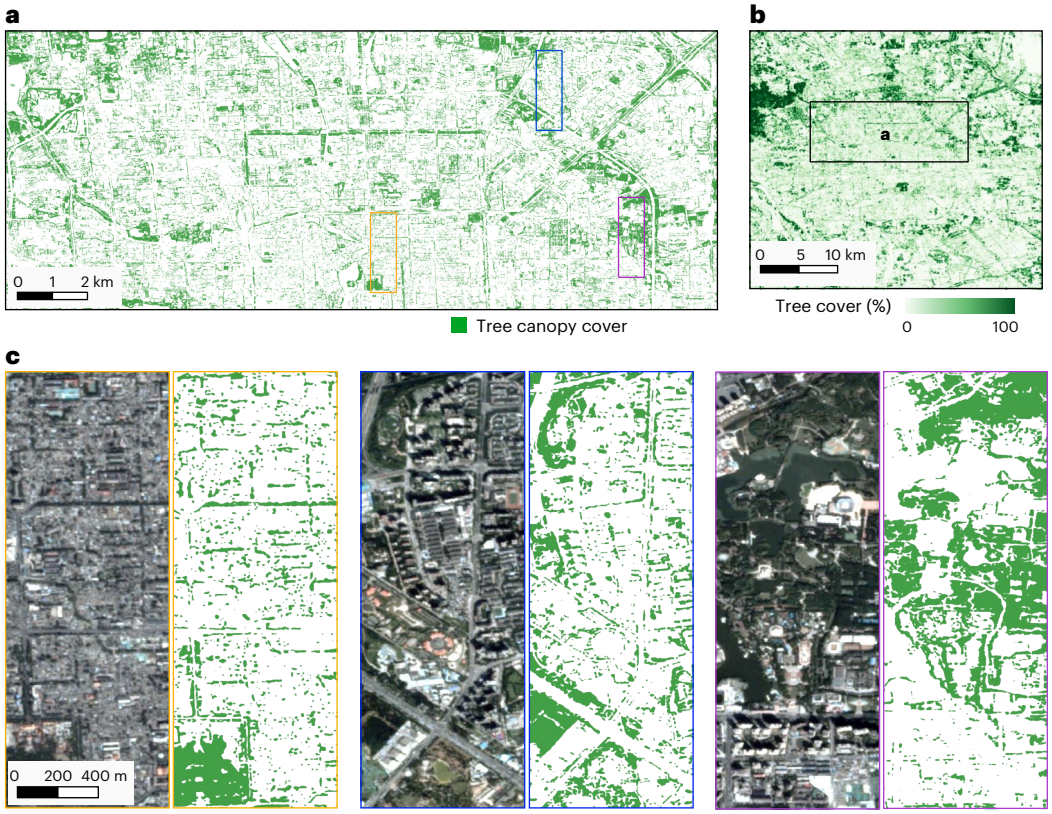

Fig. 1 | Mapping urban tree canopies in China using PlanetScope imagery from 2019. a, Trees in Beijing at 3-m resolution. **b**, Tree cover in Beijing aggregated to 1 ha (100 m × 100 m). **c**, Zoom-in of PlanetScope true-color images and urban trees mapped at 3 m from 2019.

preservation of urban trees[6,17]. Other, shorter vegetation types, such as shrubs and grasses, do not provide such benefits to the same extent[18].

Recent studies observed a considerable greening of urban areas in China over the past decade from the use of coarse resolution satellite time series[1,2]. Some studies have further documented that the greening of urban core areas has balanced vegetation losses associated with urbanization[19] and suggested that the greening of urban areas is related to greening policies[2,4]. However, a greening trend is not necessarily related to changes in tree cover, and it remains unclear whether urban tree cover has increased. This is because cities represent complex and heterogeneous landscapes where vegetation appears with a patchy structure[20]. Urban trees are often scattered irregularly, with gaps between them, and the signals from green grasses, trees, shadows and buildings are often merged in publicly available satellite images[20]. Those are characterized by a spatial resolution >10 m, limiting their applicability to map urban trees, which requires commercial, high-resolution datasets[21]. Consequently, tree cover dynamics in Chinese cities are not well quantified, and how tree cover dynamics is balanced between cities in relation to environmental conditions and urban development at the national scale is also not known.

The growing availability of submeter-resolution images from aerial campaigns or commercial satellites, such as WorldView or Gaofen-2, as well as lidar data enables monitoring of urban trees[22–25], but these images are expensive and typically not available at repeated time steps at city or national scale. This limits their applicability for large-scale urban tree mapping, and only a few countries have conducted nationwide inventories of urban trees[21,26], which moreover only represent snapshots in time. The advent of images from the PlanetScope nano-satellite constellation, which provides daily global imagery at a resolution high enough to identify single trees (~ 3–5 m), represents an emerging alternative for such large-scale mapping[21,27]. It has been shown that these images can support the mapping of individual trees at continental scales[28], but the short period of data availability (since 2017) makes them unfit to study changes over longer time periods[29]. Here, we complement the PlanetScope satellite constellation with data from RapidEye (~5 m), providing a comparable product since 2010, and uncover the changes in tree cover across major cities of China between 2010 and 2019. In contrast to previous studies[1,19], this study goes beyond the mapping of 'urban greening', by specifically targeting urban trees.

Results

Uneven distribution of urban tree cover across China's cities

We used 3-m-resolution PlanetScope satellite imagery from 2019 covering all Chinese cities with an urban area larger than 50 km^2 (242 cities; see Methods for the definition of urban areas), summing up to a total area of 51,882 km^2. We trained a deep learning segmentation model[30] with tree labels corresponding to an area of 209 km^2 (Supplementary Table 1 and Supplementary Fig. 1a) and mapped urban tree canopies, including trees along roads, in parks and in private gardens (Fig. 1) at a level of detail that was previously only possible for single-city surveys using submeter-resolution imagery[23,25] or lidar[31]. Our map can capture single trees and small tree clusters classified as 'built-up' areas in contemporary land cover products[32] (Fig. 1c and Extended Data Table 1). We find that 41.94% of the mapped trees and tree-canopy clusters were smaller than 100 m^2 (Supplementary Fig. 2), which is likely to be missed when using satellite imagery with resolution ≥10 m (Extended Data Fig. 1).

At the city level, the mean urban tree cover in the 242 large cities of China is 11.47% (model performance PlanetScope: $R^2 = 0.90$, bias of 0.37%), and a total area of 5,951 km^2 is covered by urban trees (Fig. 2 and Table 1). Urban trees are not evenly distributed among cities (Fig. 2). We grouped cities into five classes according to the city population sizes[33] (Table 1). Mega-cities have a higher mean tree cover as compared with large and medium-size cities (Table 1, Fig. 2a,b and Supplementary

https://doi.org/10.1038/s44284-025-00227-9

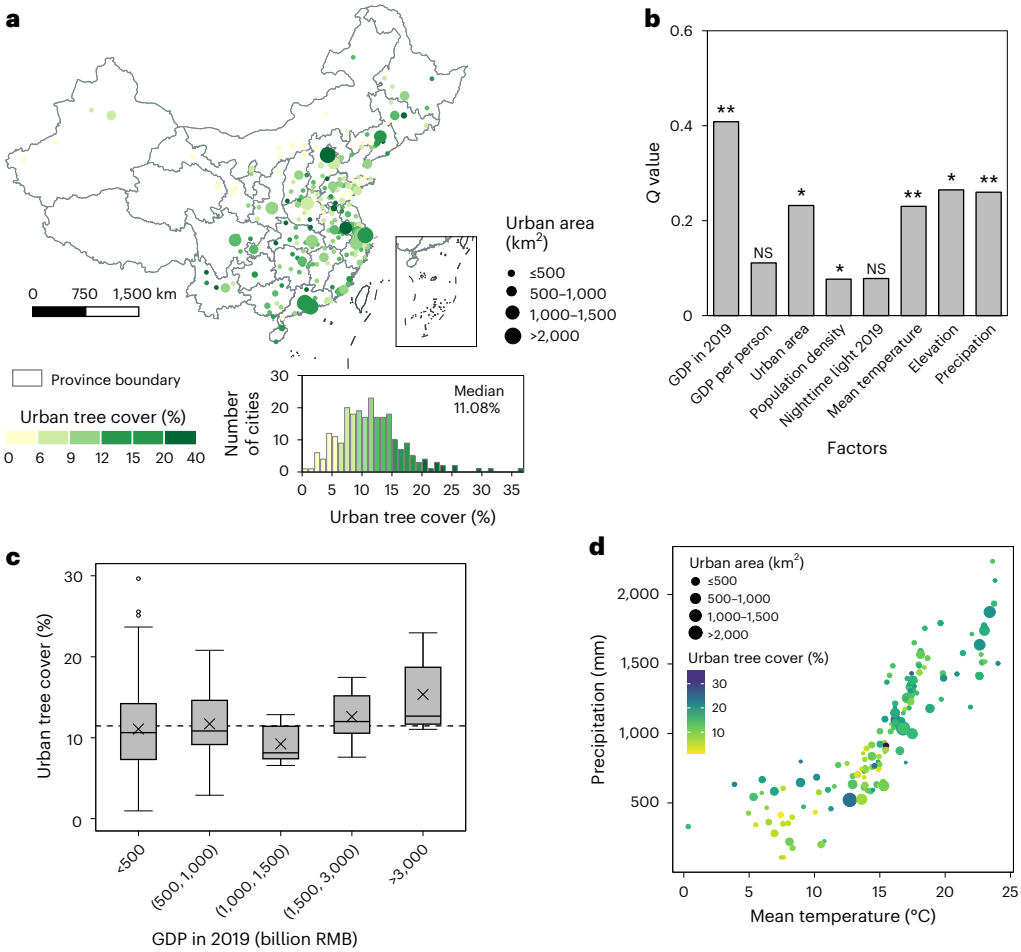

Fig. 2 | Urban tree cover at city level in 2019. a, Urban tree cover for 242 cities. Each city is represented by a circle whose size denotes the total urban area (frequency plot of urban tree cover, $n = 242$ cities). **b**, The relative importance of explanatory variables influencing the spatial pattern of urban tree cover at city level in 2019 using a factor detector analysis (Q value) (significance tested with a two-sided P value: $^{**}P \leq 0.01$; $^{*}P \leq 0.05$; NS, $P > 0.05$)[34,35]. **c**, Urban tree cover grouped by total GDP in 2019 (crosses, mean value; line, median value). In the box plots, the lower and upper box limits are the 25th and 75th percentiles, the central line is the median, and the upper (lower) whiskers extend to 1.5 and −1.5 times the interquartile range. **d**, Urban tree cover in 2019 related to annual mean temperature and annual precipitation ($n = 242$). Colors denote urban tree cover ($n = 242$ cities).

Fig. 3b): The four mega-cities Shanghai (15.80%), Beijing (22.96%), Shenzhen (17.44%) and Guangzhou (17.46%) have on average a tree cover of 18.41%, and the 11 super-large cities have on average a tree cover of 12.44%, for example, Wuhan (11.04%), Tianjin (7.01%), Nanjing (21.64%) and Foshan (11.75%) (Table 1 and Supplementary Fig. 3b). The 15 type I large cities have on average a tree cover of 11.64%, and the 31 type II large cities have an average tree cover of 11.28% (Table 1). The 180 small and medium-sized cities with a population <1 million people show the highest intraclass variability in urban tree cover, with some cities exhibiting the highest and lowest levels of urban tree cover (Table 1 and Supplementary Fig. 3). We then analyzed how different factors impact on urban tree cover using a factor detector analysis[34,35]. We found that the city-level gross domestic product (GDP) has the strongest explanatory power, surpassing the influence of GDP per person, which reflects that large and wealthy cities generally have a high tree cover (Fig. 2b,c).

Spatially, the urban tree cover varies across China, with cities in the southwest (16.70%), south-central (12.93%) and northeast (12.68%) regions having a higher urban tree cover than the national average (Supplementary Fig. 3a). On the contrary, cities in northwestern China, characterized by dry climatic conditions, show the lowest urban tree cover (6.25%) (Fig. 2a and Supplementary Figs. 3 and 4). Examples of cities with low urban tree cover are Xilingol (2.14%), Yulin (2.16%) and Aksu (2.18%), all characterized by dry climatic conditions and being located at a high elevation (Fig. 2b,d and Supplementary Fig. 4). Climatic and topographic factors, such as mean temperature and elevation, also represent important explanatory factors in the factor detector analysis[34,35] (Fig. 2b,d).

Changes in urban tree cover between 2010 and 2019

We acquired high-quality RapidEye satellite imagery for 144 representative major cities and mapped urban tree canopy cover for 2010 (the earliest phase of the lifetime of the satellite constellation) using the same deep learning framework as applied for the PlanetScope images (Methods and Extended Data Figs. 1 and 2). We report net changes (including gains and losses) in tree cover within areas that have already been urban in 2010 and also for areas that have been converted to urban from other land use types during 2010–2020 (new urban areas) (Table 1 and Fig. 3). RapidEye provides spatial resolution (~5 m) and image quality comparable to PlanetScope (~3–5 m, resampled to 3 m (ref. 29)) (Extended Data Figs. 1 and 3 and Methods), but at a less frequent revisiting time, meaning that not all the cities analyzed in 2019 could be covered in 2010 (Methods).

When considering urban boundaries from 2010, at the national scale, urban tree cover increased for 86.80% of the cities, from 7.53% (performance of the RapidEye model: $R^2 = 0.84$, bias of −0.99%) in 2010 to 13.92% in 2019 (Fig. 3a). As also observed for urban tree cover in 2019, the changes in tree cover are not homogeneous across cities and are related to the city size: The four mega-cities Shanghai

https://doi.org/10.1038/s44284-025-00227-9

Table 1 | Urban tree cover and population density in 2019 and tree cover changes (from 2010 to 2019) grouped by city population sizes[33]

Population (million persons)	Cities	2019				Change from 2010 to 2019			
		Count	Population density in 2019 (persons km^{-2})	Urban area (km^2)	Tree cover (%) (bias of 0.37%)	Count	Change in population density (persons km^{-2})	Urban area (km^2)	Tree cover (%) (bias of 1.07%)
<1	Small and medium-sized cities	181	6,350	18,950	11.28	100	732	5,949 (10,790)	4.14 (1.00)
(1, 3)	Type II large cities	31	5,453	8,733	11.08	21	768	3,547 (5,923)	5.2 (3.21)
(3, 5)	Type I large cities	15	6,681	7,818	11.64	9	1018	3,059 (4,834)	5.01 (2.53)
(5, 10)	Super-large cities	11	6,544	9,403	12.44	10	847	6589 (8,718)	0.39 (0.27)
>10	Mega-cities	4	6,605	6,574	18.41	4	989	5148 (6,575)	7.13 (6.64)
	China	**242**	**6,283**	**51,544**	**11.47**	**144**	**776**	**25,048 (36,906)**	**6.39 (4.57)**

Note that the change analysis includes fewer cities owing to the lower number of high-quality RapidEye images available in 2010. We report changes based on urban area boundaries in 2010, excluding areas that have been converted to urban during 2010–2019 (as defined in Methods), and also for urban areas in 2020 in parenthesis, which includes urban expansion areas during 2010–2020.

(9.56%), Beijing (8.68%), Shenzhen (5.12%) and Guangzhou (5.12%) have the highest increase (on average, 7.13%) (Fig. 3a and Table 1). The changes in the remaining four classes of city groups were on average lower (0.39–5.20%), with a high variability for the class covering small and medium-sized cities (Table 1 and Supplementary Fig. 4d). Urban tree cover decreased in 13.2% of all cities, for example, in Zhengzhou (−4.54%) and Tianjin (−2.44%) (Fig. 3a). Looking into new urban areas (that changed from nonurban to urban during 2010–2019), it becomes clear that the tree cover increases happened largely in areas that had already been urban in 2010 (Fig. 3b). In particular, small and medium-sized cities have seen a considerable tree cover decrease (−2.85%) in new urban areas, while areas that were already urban in 2010 show an increase in tree cover (4.14%) (Fig. 3b). Only mega-cities show a strong tree cover increase in new urban areas. The varying tree cover changes in new urban areas may be related to the land cover types that were replaced by urban expansion during 2010–2019, which was mainly cropland in the case of mega-cities (Fig. 3c and Supplementary Fig. 5).

We then studied how different factors impact urban tree cover changes (including also new urban areas) (Fig. 3d). Temperature and elevation have the strongest explanatory power for the observed changes in tree cover, surpassing the influence of GDP. This shows that geographic conditions should be considered when evaluating tree cover changes in urban areas (Fig. 3d and Supplementary Figs. 3, 4). We further compared the transition of urban tree cover from 2010 to 2019 grouped into classes of percentage tree cover for 1-ha grids (Fig. 3e and Supplementary Fig. 6). The 1-ha grids with tree cover larger than 50% have seen a slight decrease (0.45%), probably reflecting forests that were replaced by impervious surfaces. In contrast, grids with a tree cover of 0–1% in 2010 decreased by 9.45%, possibly reflecting the impact of greening activities or the transition of agricultural areas into urban areas where tree cover is higher than on the former croplands (Fig. 3b,c,e). Grids with tree cover of 1–10% increased by 4.10%, grids with 10–25% tree cover increased by 3.95% and grids with tree cover 25–50% increased by 1.85% (Fig. 3e).

Tree cover for different urban land use types

We aggregated mean tree cover for different urban land use types on the basis of land use categories from 2018[36] (Fig. 4a–d and Methods). Our results show that the highest tree cover was found in public management and service areas (20.35%), while commercial areas had the lowest tree cover (6.11%) in 2019 (Fig. 4d). Transportation areas had a mean tree cover of 11.46%, industrial areas had 9.04% and residential areas had a tree cover of 12.67% (Fig. 4d). Mega-cities have considerably more trees in public and residential areas as compared with large and small cities (Fig. 4d). Considering the diversity of residential areas, we used the year when the areas were converted from other land use forms (such as cropland) to built-up (on the basis of annual maps on impervious surface[37]), to reflect the construction year (Fig. 4b,c). When comparing the current tree cover of residential areas built in different time periods, we found that residential areas built before 1995 have a relatively low tree cover (10.98%) (Fig. 4e,f). Residential areas built after 1995 have a tree cover of 15.34%, which could be an indication of the effectiveness of urban green management implemented after 1992 (Fig. 4f). Residential areas built after 2015 have a lower tree cover (5.23%), probably because trees in newly built residential areas have not been planted or are still too small to be detected by the satellite data. Public management and service areas had the greatest increase in tree cover (+3.01%) for 2010–2019, and also commercial areas have a positive tree cover trend (+1.07%), probably due to newly established urban parks (Fig. 4g). Tree cover in transportation and industrial areas (−0.22% and −0.57%, respectively) show a decrease, reflecting that greening activities rarely target these areas (Fig. 4g).

To study the changes in tree cover within all built-up areas, we used annual maps of impervious surfaces to define the year in which areas were converted into built-up areas (Methods, Fig. 4a–c and Supplementary Figs. 7 and 8). Areas converted into built-up before 2000 saw a moderate increase in tree cover by 4% from 2010 to 2019 (Fig. 4h), while built-up areas converted between 2006 and 2010 showed a much higher increase in urban tree cover (5%). For built-up areas converted after 2010, smaller increases or even decreases in tree cover were observed, probably because trees have not been planted or are still too small to be captured by the satellite system[6,28]. Built-up areas converted after 2016 showed a loss of tree cover. These numbers suggest that tree planting can balance the initial loss of trees when built-up areas are converted from other land cover forms.

At the city level, most mega- and large cities that have experienced rapid urbanization after 2010 show an increase in urban tree cover within new built-up areas (Fig. 4j). A few large cities with new-built-up areas >100 km^2 have experienced a decrease in tree cover, including Wuhan (−2.03%), Nanchang (−0.74%), Hangzhou (−4.72%) and Chongqing (−6.28%) (Fig. 4j and Supplementary Table 2). For example, Beijing shows an increase of 7.8% in urban tree cover in new built-up areas (396 km^2), probably owing to the plantation of trees[4] (Supplementary Fig. 7). There is, however, also a number of small cities, such as Enshi (Hubei Province), which have experienced a net loss of tree cover in urban areas (−20%) without any greening (Supplementary Fig. 8).

Discussion

Urbanization in China promotes economic growth[38] and poverty reduction[39] but can at the same time cause the expansion of built-up areas and loss of natural lands[1], which challenges the sustainable development of

https://doi.org/10.1038/s44284-025-00227-9

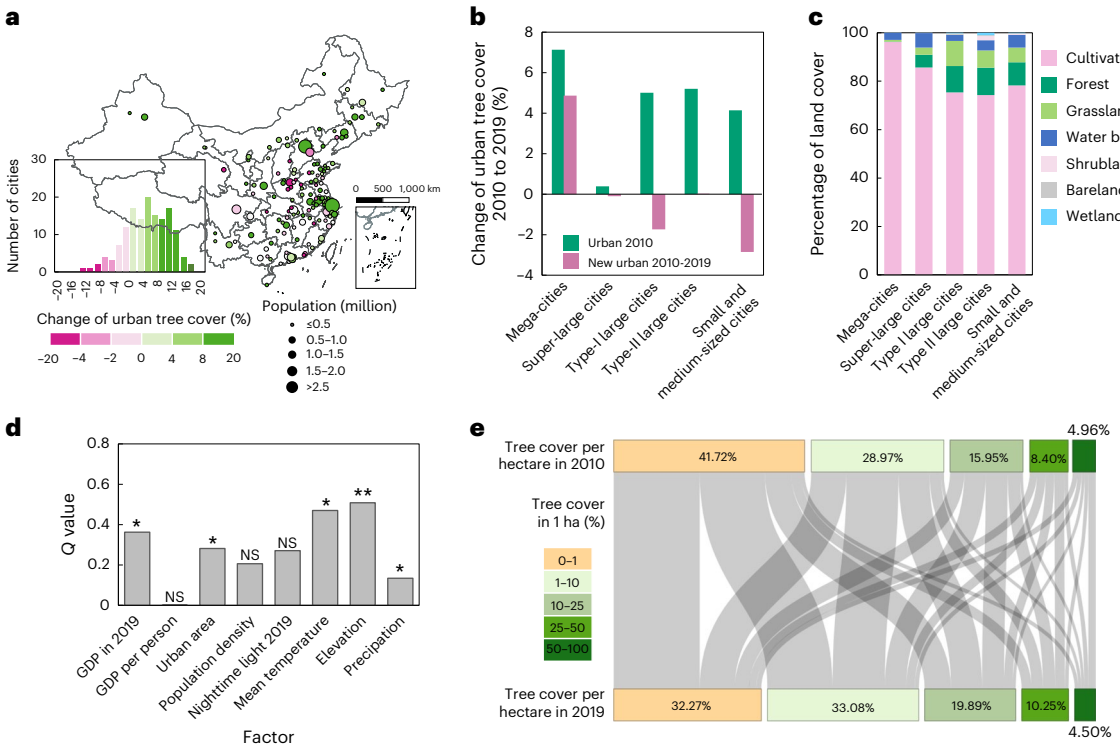

Fig. 3 | Changes in tree cover in urban areas (2010–2019). a, City-level spatial patterns and frequency plot of changes in urban tree cover for areas that were already urban in 2010 ($n = 144$). **b**, Changes in urban tree cover for areas that were already urban in 2010, and also for areas that have been converted into urban during 2010–2019 (new urban areas) for different city size groups. **c**, Loss of nonurban lands from new urban areas (2010–2020) based on GlobeLand30 land cover maps[56]. **d**, The relative importance of explanatory variables influencing the spatial pattern of changes in urban tree cover using a factor detector analysis (Q value) (significance tested with a two-sided P value: $^{**}P \leq 0.01$; $^{*}P \leq 0.05$; NS, $P > 0.05$)[34,35]. **e**, Transitions of tree cover (grouped into intervals of percentage cover per hectare) from 2010 to 2019 for 1-ha grids in urban areas ($n = 3,531,113$). Note that **d** and **e** are based on both areas that have already been urban in 2010 and new urban areas.

Chinese cities[40]. Urban trees are a key component of urban ecosystems and a possible pathway toward improved quality of life in large cities[41,42]. Consequently, the Chinese government has promoted the planting and maintenance of urban trees, aiming at mitigating the negative effects of urbanization and improving the urban environment[4].

Previous studies have shown a widespread greening of Chinese cities[1,19], based on vegetation indices such as Normalized Difference Vegetation Index (NDVI), but the somehow fuzzy variable termed 'greenness' includes also grasses and shrubs[19]. Greenness maps derived from vegetation indices lack units and are less well suited for quantifying changes, being merely indicative for reporting directions of change. However, NDVI has often been used as a proxy for suggesting changes in urban tree cover[43–45]. Interestingly, when comparing greenness changes (reflected by Moderate-Resolution Imaging Spectroradiometer (MODIS) NDVI) with tree cover changes during 2010–2019, we find a weak relationship ($r^2 = 0.10$), indicating the limited use of greenness as a proxy for urban tree cover changes (Supplementary Fig. 9), and also high resolution Sentinel-2-based NDVI does not correlate well with our tree cover maps at the city scale (Supplementary Fig. 10). Our tree cover maps for 2010 and 2019 show a clear increase in tree cover, probably as a consequence of urban tree plantations (Extended Data Figs. 2 and 4), but we also reveal that large cities, and in particular mega-cities, have a considerably higher tree cover and tree cover increase as compared with the majority of cities in China. Our results indicate that economic differences, but also climate and topography, determine differences in tree cover, which was also observed at a global scale[46]. Developed and wealthy regions, such as many cities in North America and Europe (or more generally, the Global North), have made substantial investments in the planting and maintenance of urban trees[47,48], which arguably has improved the well-being of residents[49,50]. In contrast, many densely populated cities, often located in the Global South, have limited resources for maintaining or increasing tree cover, which impacts people's health, for example, via heatwaves[51]. These effects are aggravated by climatic conditions: in dryer regions, the costs of planting and managing urban trees is higher, but at the same time, the health benefits, such as the cooling effect, are more urgently needed[52]. Moreover, relative increases in tree cover may also be related to the rate of urban expansion of a city during 2010–2019 (Fig. 4j). The net decline in tree cover in some cities is probably related to new urban areas where trees that were potentially planted have not yet reached a size that makes them detectable by the satellite data used[6,28].

While the apparent success story of increased tree cover in China's cities is notable, a comprehensive evaluation of the sustainability of urban tree management must consider the uneven distribution and the influence of geographic and climate factors. Our study found that the explanatory power of relative GDP is lower than that of the total GDP, which indicates that increasing urban tree cover is not to the same extent a priority of smaller wealthy cities as compared with large cities. This concurs with the fact that larger cities exhibit the most pronounced challenges associated with urban heat islands, marked by elevated daytime temperatures, reduced nighttime cooling and higher levels of air pollution. To address these issues, a potential mitigation strategy involves augmenting tree cover within urban areas. Additionally, our research reveals a considerable variability in tree cover among emerging cities, a phenomenon partially influenced by climatic and geographic conditions. In particular, the low tree cover in northwestern China, predominantly in developing medium and small cities, may be attributed to the substantial costs associated with

https://doi.org/10.1038/s44284-025-00227-9

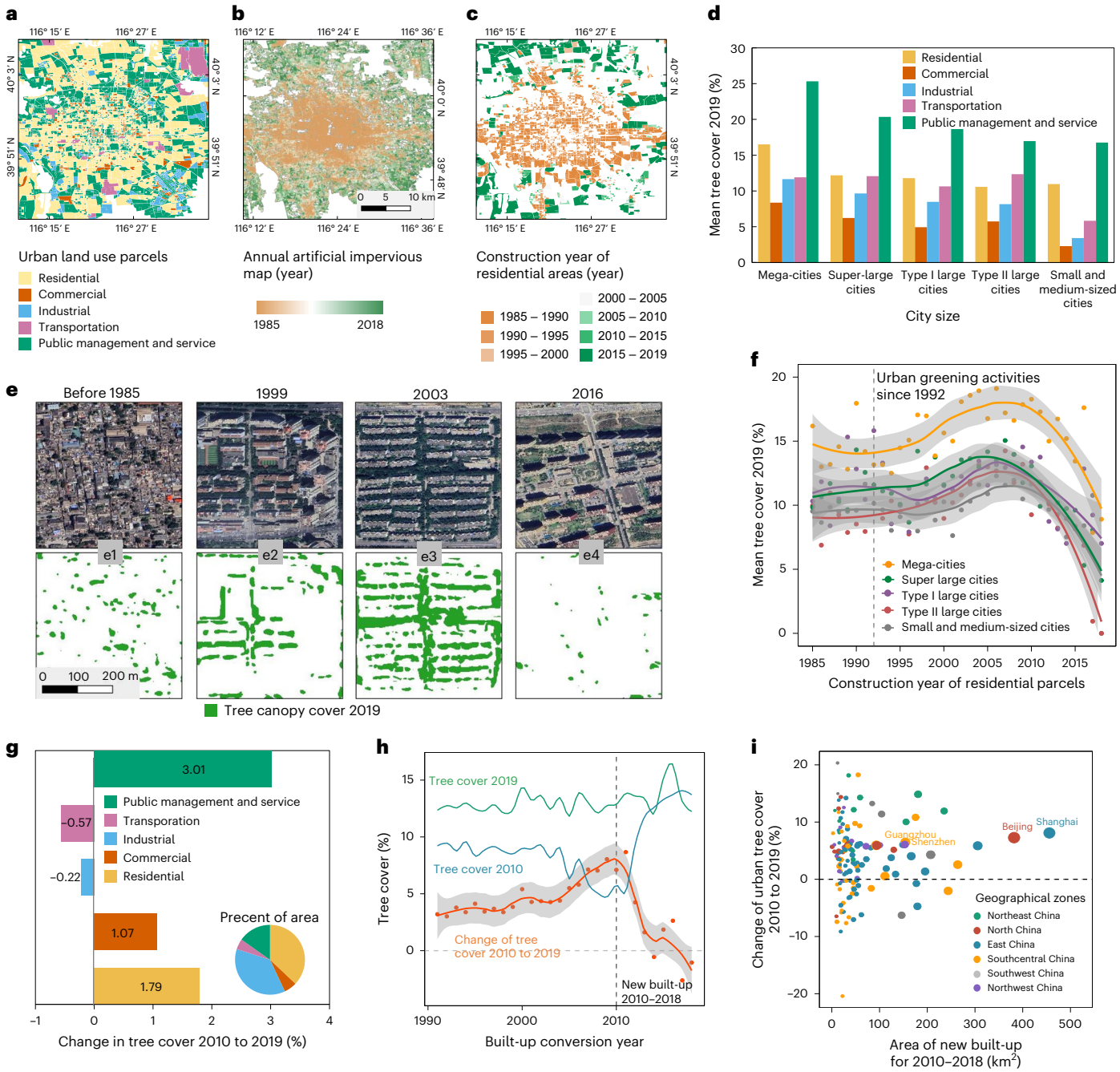

Fig. 4 | Urban tree cover related to urban land use types in China. a, Urban land use categories (EULUC-China[36]), using Beijing as an example. **b**, Annual artificial impervious areas for 1985–2018 from the GAIA product[37]. **c**, Construction year of residential areas (Methods). **d**, Mean tree cover in 2019 for different urban land use types grouped by city size[33]. **e**, Examples of residential areas built in different periods: before 1985 (e1), 1999 (e2), 2003 (e3) and 2016 (e4), illustrated by very-high-resolution satellite images (WorldView, 2024 Maxar Technologies) and tree canopy cover for 2019. **f**, Mean tree cover in residential areas in China during 1985–2018, grouped by construction year. The fit lines were fit by scatterplot smoothing (LOESS), and the shaded areas indicates the 95% confidence interval for the LOESS estimate. **g**, Tree cover changes for 2010–2019 for different urban land use types. **h**, Mean tree cover for areas of different construction years (that is, conversion from other land use into urban built-up) during 1991–2018. The fit orange line and confidence areas (gray color, 95%) were fit by the LOESS function. **i**, Changes in tree cover and new built-up areas for 2010–2019 at the city level ($n = 144$). Colors denote geographical zones. Mega-cities are labeled with city names.

planting and managing urban trees in these dry regions, for example, owing to expenses related to irrigation[53]. Therefore, in arid regions, it is advisable to select drought-tolerant tree species or implement alternative strategies such as incorporating short vegetation to ensure sustainable greening practices. With global warming, the maintenance costs associated with irrigation might increase, which may require the use of natural-based solutions that are adapted to the local climate and the preservation of existing trees[54]. In response to these issues, the Chinese government released new guidelines on the development of nature-based solutions for urban parks and forests in 2021, which emphasize the importance of natural-based planning and implementing rainwater harvesting for irrigation as important components of urban green management[55].

Uncertainty within our study pertains to several factors. First, the definition of urban areas is based on continuous built-up areas using a previously published land cover map[56]. The definition may

exclude subcenters or outskirt towns, which could lead to different values from our study as compared with national statistics that base calculations on urban tree cover using administrative borders. Second, the current tree cover change maps are only based on satellite data from two years (2010 and 2019) and therefore do not provide annual information that would give more detailed insights into the effects of urban tree management. The tree cover assessments for these two years were conducted by different satellite remote sensing systems, and a thorough intercomparison showed that there is no systematic bias between the sensor systems. While the availability of the satellite data used is lower before 2019, newer PlanetScope satellites now provide daily images, allowing for a continuation of this work and a consistent monitoring of annual urban tree cover after 2019. Third, the use of this type of optical images limits the analyses to the metric of tree cover, which does not provide information on tree size and species, which is however important in regards to the ecological services provided[57]. Finally, shadows cast by tall buildings may reduce the detectability of trees to some extent. The inclusion of lidar, drone and field data is essential to enhance the mapping accuracy and leverage further information on urban trees. Future research should further examine the driving mechanisms and consider various socioeconomic factors, local climate zones and urban growth patterns.

Our study is based on commercial imagery, and the costs of repeated analyses at the national level are currently not negligible for a large-sized country such as China. However, the spatial resolution and coverage of publicly available data sources are not yet sufficient for mapping trees as single objects, often leaving a high uncertainty on mapping urban tree cover and in particular changes thereof. Nevertheless, the costs of nanosatellite images are considerably lower as compared with traditional commercial submeter-resolution imagery, and our study demonstrates that current technologies enable comprehensive monitoring of tree cover changes not only in Chinese cities but worldwide. This is expected to facilitate evidence-based decision-making and foster global collaboration in urban greening initiatives for different countries as pledged by the 11th UN Sustainable Development Goal (sustainable cities and communities) advocating for creating green public spaces[58].

Methods

To calculate the change in urban tree cover over the past decades, we defined urban areas from a land cover map and selected the major 242 cities in China. We then mapped urban tree canopies using PlanetScope images from 2019 and RapidEye images from 2010 using a deep learning framework and compared the dynamics of urban trees between cities, as well as for various urban land use types.

Defining urban areas

We selected 242 cities by their size (area ≥50 km^2), using the 'artificial surface' class from the GlobeLand30 land cover map in 2020 provided at 30 m spatial resolution[56]. Areas classified as grassland and forest within built-up areas were included as urban areas. We also use Google Earth satellite imagery to double-check all urban boundaries, reviewing misclassifications and confirming the urban areas as spatially continuous built-up areas. Shijiazhuang City was omitted owing to the lack of high-quality PlanetScope images for 2019. We then classified the cities into five population size groups according to the latest standard released by China's State Council in 2014[33] (Table 1 and Extended Data Fig. 5), including 4 mega-cities (population ≥10 million), 11 super-large cities (population ≥5 million), 15 type I large cities (population ≥3 million), 31 type II large cities (population ≥1 million) and 181 small and medium-sized cities (population <1 million) (Table 1 and Extended Data Fig. 5). The cities were divided into six geographical zones to compare the regional differences in urban tree cover: northeast China (23 cities), north China (28 cities), east China (99 cities), south-central China (63 cities), northwest China (18 cities) and southwest China (11 cities) (Extended Data Fig. 5). High-quality RapidEye images from around 2010 covering 144 cities were used to study changes in urban tree cover. These cities are representative for all climatic conditions, geographical zones and different stages of cities (Extended Data Fig. 5). The same urban boundaries from 2020 were used to compare the net change of tree cover. Moreover, we also defined urban areas in 2010 on the basis of the built-up areas from the GlobeLand30 land cover map[56] in 2010. We then compared the change in tree cover in areas that were already urban in 2010 and new urban areas, that is, areas converted from non-urban into urban land use during 2010–2020 (Supplementary Fig. 11).

Preprocessing PlanetScope and RapidEye images

We use PlanetScope images (four bands: red, green, blue and near-infrared) at 3 m spatial resolution[29] to generate annual composites for 242 cities in 2019. The images were acquired during a phenological window where trees have green leaves but grasses have passed their productivity peak, which is defined using the MODIS phenology product. For more details, see ref. 28. We organized and mosaicked raw satellite scenes in grids of 1° × 1° (ref. 28). We then upsampled Planet images from 3 m to 1 m using bilinear interpolation to preserve the high quality of the manual training samples and smooth the boundaries of tree canopies[28].

The RapidEye images have a spatial resolution of ~5 m and are acquired in five spectral bands, including blue, green, red, red-edge and near-infrared. We used RapidEye images from around 2010, preprocessed in the same manner as the PlanetScope images. Owing to the lack of reliable metadata on cloud cover, we only kept cloud-free RapidEye imagery for 144 cities by visually screening the images and disregarding cities with low data quality. Furthermore, a few patches within urban areas that had no available observations from either PlanetScope in 2019 or RapidEye in 2010 were also excluded from the analysis. This was done to ensure a consistent comparison of changes in tree cover within urban areas.

Segmentation of tree canopies using deep learning

We used the framework from refs. 30,28 to segment tree canopy cover using a convolutional neural network, specifically the U-Net architecture. We trained two models, one for PlanetScope and one for RapidEye. The models were trained with a batch size of 32 and a patch size of 256 × 256 pixels, and the Tversky loss was used as the loss function to balance the commission (60%) and omission errors (40%) (see Supplementary Table 1 for specific settings). The training labels included individual tree crowns and clusters of trees and covered 209.29 km^2 over 496 sample sites for 2019, including 34.74 km^2 of trees distributed across 69 cities (Supplementary Fig. 1a and Supplementary Table 1). For the 2010 RapidEye data, we delineated tree canopies for 481 sites, covering 74.15 km^2 across 57 cities (Supplementary Fig. 1b and Supplementary Table 1) and trained a model in the same way as was done for PlanetScope.

Evaluation and comparison

We compared our maps with an evaluation dataset consisting of 185 randomly selected 100 × 100 m patches with manual labels from PlanetScope and RapidEye images (Extended Data Fig. 6). The data used for evaluation were not used for training the models or selecting the hyperparameters. The PlanetScope model showed an overall accuracy of 0.90, a kappa coefficient of 0.85, a mean absolute error (MAE) of 0.37% and a root mean square error (RMSE) of 7.69% (Extended Data Fig. 6a–c,f). The RapidEye model achieved an overall accuracy of 84%, a kappa coefficient of 0.78, an MAE of −0.99% and an RMSE of 9.84% (Extended Data Fig. 6a,b,d,g). To evaluate the uncertainty of the change between RapidEye and PlanetScope, we manually labeled changes between 2010 and 2019 for 185 patches and compared the results with the model predictions. Here, we obtained an R^2 of 0.83, an MAE of 1.07% and an RMSE of 8.99% (Extended Data Fig. 6e), suggesting

that the intercomparison of tree cover maps derived from two different satellite systems is valid. The validation shows higher accuracy in areas with larger canopy cover compared with those areas with lower canopy cover (Extended Data Fig. 6). Urban forests, with their larger canopy areas, can be mapped with lower uncertainty than smaller, irregularly scattered trees. We collected high-quality RapidEye images from 2019 for six selected cities to study whether there are systematic differences between tree cover maps derived from PlanetScope and RapidEye imagery, which would lead to biased change values for 2010–2019 (Extended Data Figs. 1 and 3 and Supplementary Table 3). The results show that there is no obvious systematic bias (2.39%; Supplementary Table 3).

We compared our tree cover map in 2019 with other tree cover maps, including the MODIS Vegetation Continuous Fields Yearly Global 250m (MOD44B version 6) tree cover product[54] and the European Space Agency (ESA) WorldCover 2020 tree cover map[32]. Our map showed that MOD44B (spatial resolution of 250 m) underestimated tree cover in cities by 9.52% (Extended Data Fig. 7a). The mean urban tree cover of the Sentinel-2-based WorldCover map from 2020 was only 0.66% lower as compared with our map, but areas of low tree cover were underestimated while areas of higher tree cover were overestimated (Extended Data Fig. 7b). The results showed that 6.79% of the tree cover in built-up areas was misclassified in the ESA WorldCover 2020 map (covering a total of 2,182.12 km^2 of urban areas in our study) (Extended Data Table 1). The trees omitted by the ESA map are often located in densely built-up areas, dominated by small and isolated trees. Additionally, almost half of the areas in the class 'tree cover' were found to be misclassified, as it was found to be dominated by shrubland, or grassland (Extended Data Table 1). The Esri land cover map[59] underestimate urban tree cover, especially in the case of scattered trees (Extended Data Fig. 1).

Urban tree cover for different urban land use types

We used the urban land use category map from 2018 covering the whole of China (EULUC-China[36]) to define different types of urban land use. This map combines multiple datasets, including 10-m satellite images, OpenStreetMap, nighttime lights, points of interest (POI) and Tencent social big data[36]. EULUC-China classifies urban land into five classes: residential, commercial, industrial, transportation, and public management and service[36]. Public management and service areas include land used for administrative purposes, education, hospitals, public sports, cultural services, parks and green spaces. We examined the distribution and change in urban tree cover for different urban land use types. We further defined the year when residential areas were converted from other land use types (such as cropland) using the annual maps of artificial impervious surface areas (GAIA)[37] (Fig. 4 and Supplementary Figs. 6 and 7). We then assessed the urban tree cover in 2019 and the change from 2010 to 2019 for residential areas grouped by the year they were converted.

Development stages of built-up areas

Annual maps of global artificial impervious surface areas (GAIA) for 1985–2018[37] at 30 m resolution were used to identify in which year areas were converted into built-up areas in 144 cities. The built-up areas continuously expanded over the past decades, thereby indicating in a spatially explicit way the expansion of newly constructed built-up areas (Supplementary Figs. 6 and 7). The different starting years when first observed as built-up serve as an indicator of the development stage of built-up areas. The mean tree cover in 2010 and 2019 for annual new built-up areas was studied to compare the tree cover change in built-up areas at various development stages.

Other datasets and factor detector analysis

We used GlobeLand30 (2010 and 2020)[56] to estimate the loss of non-urban lands to new urban areas between 2010 and 2020. We used the WorldPop population density maps[60] from 2019 and 2010 to quantify the population size for each city and changes in population density. WorldPop provides the estimated number of people residing in a 1 × 1-km grid on the basis of a random forest model and a global dataset including administrative unit-based census information, which has a higher spatial resolution and update frequency than other population datasets[60]. The yearly precipitation and mean temperature datasets are derived from the TerraClimate precipitation dataset for the period 1970–2015. The elevation for each city was calculated from the Shuttle Radar Topography Mission version 3 product[61] at a resolution of 1 arc-sec (~30 m). The mean nighttime light map for 2019 was derived from monthly nighttime data from the Visible Infrared Imaging Radiometer Suite day/night band[62] at 500 m spatial resolution. To indicate the economic conditions, the total GDP of each city in 2019 was collected from the Chinese Statistical Yearbook. We use the *Q* value of each factor from a factor detector analysis[35] to quantify their relative importance for explaining urban tree cover in 2019 and changes in tree cover from 2010 to 2019. The geographical detector model was used to analyze influencing factors, including spatially correlated variables[63,64]. In this study, we included GDP for 2019, GDP per capita, urban areas and population size as socioeconomic factors, while mean temperature and mean precipitation for each city were included as climate factors to assess both the effects of urban tree cover in 2019 and the changes in urban tree cover between 2010 and 2019. The optimal parameters-based geographical detector model[34] was used to automatically select the best way of stratifying the continuous values of the variables, including equal distribution, natural breaks, quantile interval, geometric interval and standard deviation interval. We then estimated the importance of multiple factors with the stratified variables by using the factor detector approach. Higher *Q* values indicate greater importance in explaining urban tree cover and its changes.

Reporting summary

Further information on research design is available in the Nature Portfolio Reporting Summary linked to this article.

Data availability

The high-resolution tree canopy and changes in tree cover are available at https://ee-xzrscph.projects.earthengine.app/view/china-urban-tree-change. PlanetScope imagery and RapidEye imagery in urban areas over China are available via Planet Labs at https://www.planet.com/products/ upon acquiring a license agreement. The GlobeLand30 land cover dataset (2010 and 2020) is available at http://www.globallandcover.com/home_en.html. The ESA WorldCover 2020 land cover map is available at https://worldcover2020.esa.int/. Annual maps for the global artificial impervious areas (GAIA) dataset are available at http://data.ess.tsinghua.edu.cn. The essential urban land use categories map in China (EULUC-China) is available at http://data.ess.tsinghua.edu.cn/. VIIRS-DNB nighttime light is available via the Google Earth Engine at https://developers.google.com/earth-engine/datasets/catalog/NOAA_VIIRS_DNB_MONTHLY_V1_VCMCFG. GDP data are accessible from the National Bureau of Statistics of the People's Republic of China. Population density data from WorldPop in 2019 are available at https://www.worldpop.org. The administrative boundaries in China are available via the national catalog service for geographic information at https://www.ngcc.cn/.

Code availability

The code for the tree canopy detection framework based on U-Net is available via Zenodo at https://doi.org/10.5281/zenodo.3978185 (ref. 65).

References

1. Liu, X. et al. High-spatiotemporal-resolution mapping of global urban change from 1985 to 2015. *Nat. Sustain.* https://doi.org/10.1038/s41893-020-0521-x (2020).

2. Zhang, X. et al. A large but transient carbon sink from urbanization and rural depopulation in China. *Nat. Sustain.* **5**, 321–328 (2022).
3. Folberth, G. A., Butler, T. M., Collins, W. J. & Rumbold, S. T. Megacities and climate change—a brief overview. *Environ. Pollut.* **203**, 235–242 (2015).
4. Feng, D., Bao, W., Yang, Y. & Fu, M. How do government policies promote greening? Evidence from China. *Land Use Policy* **104**, 105389 (2021).
5. Wang, C., Jin, J., Davies, C. & Chen, W. Y. Urban forests as nature-based solutions: a comprehensive overview of the national forest city action in China. *Curr. For. Rep.* **10**, 119–132 (2024).
6. Yao, N. et al. Beijing's 50 million new urban trees: strategic governance for large-scale urban afforestation. *Urban For. Urban Green.* **44**, 126392 (2019).
7. Jackson, L. E. The relationship of urban design to human health and condition. *Landsc. Urban Plan.* **64**, 191–200 (2003).
8. Endreny, T. A. Strategically growing the urban forest will improve our world. *Nat. Commun.* **9**, 1160 (2018).
9. Schwaab, J. et al. The role of urban trees in reducing land surface temperatures in European cities. *Nat. Commun.* **12**, 6763 (2021).
10. Iungman, T. et al. Cooling cities through urban green infrastructure: a health impact assessment of European cities. *Lancet* **401**, 577–589 (2023).
11. Ko, Y. Trees and vegetation for residential energy conservation: a critical review for evidence-based urban greening in North America. *Urban For. Urban Green.* **34**, 318–335 (2018).
12. Nowak, D. J. & Crane, D. E. Carbon storage and sequestration by urban trees in the USA. *Environ. Pollut.* **116**, 381–389 (2002).
13. Locosselli, G. M. et al. The role of air pollution and climate on the growth of urban trees. *Sci. Total Environ.* **666**, 652–661 (2019).
14. Zhang, B., Xie, G., Zhang, C. & Zhang, J. The economic benefits of rainwater-runoff reduction by urban green spaces: a case study in Beijing, China. *J. Environ. Manage.* **100**, 65–71 (2012).
15. Wang, J. et al. Significant effects of ecological context on urban trees' cooling efficiency. *ISPRS J. Photogramm. Remote Sens.* **159**, 78–89 (2020).
16. Alvey, A. A. Promoting and preserving biodiversity in the urban forest. *Urban For. Urban Green.* **5**, 195–201 (2006).
17. Eisenman, T. S., Flanders, T., Harper, R. W., Hauer, R. J. & Lieberknecht, K. Traits of a bloom: a nationwide survey of US urban tree planting initiatives (TPIs). *Urban For. Urban Green.* **61**, 127006 (2021).
18. Edmondson, J. L., Stott, I., Davies, Z. G., Gaston, K. J. & Leake, J. R. Soil surface temperatures reveal moderation of the urban heat island effect by trees and shrubs. *Sci. Rep.* **6**, 33708 (2016).
19. Zhang, X. et al. Urban core greening balances browning in urban expansion areas in china during recent decades. *J. Remote Sens.* **4**, 0112 (2024).
20. Shahtahmassebi, A. R. et al. Remote sensing of urban green spaces: a review. *Urban For. Urban Green.* **57**, 126946 (2021).
21. Liu, S. et al. The overlooked contribution of trees outside forests to tree cover and woody biomass across Europe. *Sci. Adv.* **9**, eadh4097 (2023).
22. Yadav, S., Rizvi, I. & Kadam, S. Urban tree canopy detection using object-based image analysis for very high resolution satellite images: a literature review. In *Proc. 2015 International Conference on Technologies for Sustainable Development* (ICTSD) 1–6 (ICTSD, 2015); https://doi.org/10.1109/ICTSD.2015.7095889
23. Pu, R. & Landry, S. A comparative analysis of high spatial resolution IKONOS and WorldView-2 imagery for mapping urban tree species. *Remote Sens. Environ.* **124**, 516–533 (2012).
24. Pu, R. & Landry, S. Mapping urban tree species by integrating multi-seasonal high resolution pléiades satellite imagery with airborne LiDAR data. *Urban For. Urban Green.* **53**, 126675 (2020).
25. Erker, T., Wang, L., Lorentz, L., Stoltman, A. & Townsend, P. A. A statewide urban tree canopy mapping method. *Remote Sens. Environ.* **229**, 148–158 (2019).
26. Guo, J., Xu, Q., Zeng, Y., Liu, Z. & Zhu, X. X. Nationwide urban tree canopy mapping and coverage assessment in Brazil from high-resolution remote sensing images using deep learning. *ISPRS J. Photogramm. Remote Sens.* **198**, 1–15 (2023).
27. Brandt, M. et al. Severe decline in large farmland trees in India over the past decade. *Nat. Sustain.* **7**, 860–868 (2024).
28. Reiner, F. et al. More than one quarter of Africa's tree cover is found outside areas previously classified as forest. *Nat. Commun.* **14**, 2258 (2023).
29. Roy, D. P., Huang, H., Houborg, R. & Martins, V. S. A global analysis of the temporal availability of PlanetScope high spatial resolution multi-spectral imagery. *Remote Sens. Environ.* **264**, 112586 (2021).
30. Brandt, M. et al. An unexpectedly large count of trees in the West African Sahara and Sahel. *Nature* **587**, 78–82 (2020).
31. Ma, Q. et al. Individual structure mapping over six million trees for New York City, USA. *Sci. Data* **10**, 102 (2023).
32. Daniele, Z. et al. ESA WorldCover 10 m 2020 v100 dataset. *Zenodo* https://doi.org/10.5281/zenodo.5571936 (2021).
33. The State Council of People's Republic of China. Notice on adjusting the standard of city size (in Chinese). *Government of China* http://www.gov.cn/zhengce/content/2014-11/20/content_9225.htm (2014).
34. Song, Y., Wang, J., Ge, Y. & Xu, C. An optimal parameters-based geographical detector model enhances geographic characteristics of explanatory variables for spatial heterogeneity analysis: cases with different types of spatial data. *GIScience Remote Sens.* **57**, 593–610 (2020).
35. Wang, J. et al. Geographical detectors-based health risk assessment and its application in the neural tube defects study of the Heshun Region, China. *Int. J. Geogr. Inf. Sci.* **24**, 107–127 (2010).
36. Gong, P. et al. Mapping essential urban land use categories in China (EULUC-China): preliminary results for 2018. *Sci. Bull.* **65**, 182–187 (2020).
37. Gong, P. et al. Annual maps of global artificial impervious area (GAIA) between 1985 and 2018. *Remote Sens. Environ.* **236**, 111510 (2020).
38. Chen, M., Zhang, H., Liu, W. & Zhang, W. The global pattern of urbanization and economic growth: evidence from the last three decades. *PLoS ONE* **9**, e103799 (2014).
39. Zhang, Y. *Urbanization, Inequality, and Poverty in the People's Republic of China*. ADBI Working Paper 584 (Asian Development Bank Institute, 2016).
40. He, C., Gao, B., Huang, Q., Ma, Q. & Dou, Y. Environmental degradation in the urban areas of China: evidence from multi-source remote sensing data. *Remote Sens. Environ.* **193**, 65–75 (2017).
41. Roloff, A. *Urban Tree Management: for the Sustainable Development of Green Cities* (Wiley, 2016).
42. Tang, L., Shao, G. & Groffman, P. M. Urban trees: how to maximize their benefits for humans and the environment. *Nature* **626**, 261–261 (2024).
43. Timilsina, S., Aryal, J. & Kirkpatrick, J. B. Mapping urban tree cover changes using Object-Based Convolution Neural Network (OB-CNN). *Remote Sens.* **12**, 3017 (2020).
44. Ossola, A. & Hopton, M. E. Measuring urban tree loss dynamics across residential landscapes. *Sci. Total Environ.* **612**, 940–949 (2018).
45. Wallace, L. et al. Linking urban tree inventories to remote sensing data for individual tree mapping. *Urban For. Urban Green.* **61**, 127106 (2021).

46. Leng, S., Sun, R., Yang, X. & Chen, L. Global inequities in population exposure to urban greenspaces increased amidst tree and nontree vegetation cover expansion. *Commun. Earth Environ.* **4**, 1–10 (2023).
47. Kroeger, T., McDonald, R. I., Boucher, T., Zhang, P. & Wang, L. Where the people are: Current trends and future potential targeted investments in urban trees for PM10 and temperature mitigation in 27 US cities. *Landsc. Urban Plan.* **177**, 227–240 (2018).
48. Wild, T., Freitas, T. & Vandewoestijne, S. *Nature-Based Solutions: State of the Art in EU-Funded Projects* (Publications Office of the European Union, 2020).
49. Morani, A., Nowak, D. J., Hirabayashi, S. & Calfapietra, C. How to select the best tree planting locations to enhance air pollution removal in the MillionTreesNYC initiative. *Environ. Pollut.* **159**, 1040–1047 (2011).
50. Nowak, D. J., Hirabayashi, S., Bodine, A. & Greenfield, E. Tree and forest effects on air quality and human health in the United States. *Environ. Pollut.* **193**, 119–129 (2014).
51. Yang, J. et al. Heatwave and mortality in 31 major Chinese cities: definition, vulnerability and implications. *Sci. Total Environ.* **649**, 695–702 (2019).
52. Manoli, G. et al. Magnitude of urban heat islands largely explained by climate and population. *Nature* **573**, 55–60 (2019).
53. Luketich, A. M., Papuga, S. A. & Crimmins, M. A. Ecohydrology of urban trees under passive and active irrigation in a semiarid city. *PLoS ONE* **14**, e0224804 (2019).
54. Van den Bosch, M. & Sang, Å. O. Urban natural environments as nature-based solutions for improved public health—a systematic review of reviews. *Environ. Res.* **158**, 373–384 (2017).
55. Qi, J. J. & Dauvergne, P. China and the global politics of nature-based solutions. *Environ. Sci. Policy* **137**, 1–11 (2022).
56. Chen, J. et al. Global land cover mapping at 30m resolution: A POK-based operational approach. *ISPRS J. Photogramm. Remote Sens.* **103**, 7–27 (2015).
57. Choudhury, M. A. M. et al. Urban tree species identification and carbon stock mapping for urban green planning and management. *Forests* **11**, 1226 (2020).
58. United Nations. *Transforming Our World: the 2030 Agenda for Sustainable Development* (United Nations, 2015).
59. Karra, K. et al. Global land use/land cover with Sentinel-2 and deep learning. In *IGARSS 2021: 2021 IEEE International Geoscience and Remote Sensing Symposium*; 2021 July, Brussels, Belgium, 4704–4707 (IEEE, 2021).
60. Tatem, A. J. WorldPop, open data for spatial demography. *Sci. Data* **4**, 170004 (2017).
61. Farr, T. G. et al. The Shuttle radar topography mission. *Rev. Geophys.* **45**, 2 (2007).
62. Elvidge, C. D., Zhizhin, M., Ghosh, T., Hsu, F.-C. & Taneja, J. Annual time series of global VIIRS nighttime lights derived from monthly averages: 2012 to 2019. *Remote Sens.* **13**, 922 (2021).
63. Wu, Y., Hu, K., Han, Y., Sheng, Q. & Fang, Y. Spatial characteristics of life expectancy and geographical detection of its influencing factors in China. *Int. J. Environ. Res. Public. Health* **17**, 906 (2020).
64. Lin, Q. & Wang, Y. Spatial and temporal analysis of a fatal landslide inventory in China from 1950 to 2016. *Landslides* **15**, 2357–2372 (2018).
65. Ankit. ankitkariryaa/An-unexpectedly-large-count-of-trees-in-the-western-Sahara-and-Sahel: Paper version. *Zenodo* https://doi.org/10.5281/zenodo.3978185 (2020).

Acknowledgements

X.Z. was funded by the China Scholarship Council (grant no. 201904910835). M.B. was funded by the European Research Council under the European Union's Horizon 2020 Research and Innovation Programme (grant no. 947757 TOFDRY) and DFF Sapere Aude (grant no. 9064–00049B). Xiaowei Tong was funded by the National Natural Science Foundation of China for Excellent Young Scientists (Overseas) and the National Natural Science Foundation of China (42371129). F.T. acknowledges funding from the National Natural Science Foundation of China (grant no. 42001299) and the Seed Fund Program of the Sino–Foreign Joint Scientific Research Platform of Wuhan University (grant no. WHUZZJJ202205). Y.Y. was funded by the International Partnership Program of the Chinese Academy of Sciences (grant no. 092GJHZ2022029GC) and the CAS Interdisciplinary Innovation Team (grant no. JCTD-2021-16). B.C. acknowledges support from the Research Grants Council of Hong Kong (grant nos. HKU27600222 and HKU17601423), the NSFC/RGC Joint Research Scheme (grant no. N_HKU722/23) and the National Key Research and Development Program of China (grant no. 2022YFB3903703). X.X. was supported by the US National Science Foundation (grant nos. 1911955 and 2200310). R.F. acknowledges support from Villum Fonden through the project Deep Learning and Remote Sensing for Unlocking Global Ecosystem Resource Dynamics (DeReEco, grant no. 34306).

Author contributions

X.Z. and M.B. designed the research. X.Z., M.B., Xiaoye Tong and F.R. helped to collect PlanetScope and RapidEye images, and F.R. and S.L. developed the code for the deep learning pipeline. X.Z. prepared the annotation data and conducted the analysis. X.Z., M.B., W. Zhang and R.F. drafted the first manuscript. Xiaowei Tong, F.T., Y.Y., W. Zhou, B.C. and X.X. reviewed the manuscript.

Competing interests

The authors declare no competing interests.

Additional information

Extended data is available for this paper at https://doi.org/10.1038/s44284-025-00227-9.

Supplementary information The online version contains supplementary material available at https://doi.org/10.1038/s44284-025-00227-9.

Correspondence and requests for materials should be addressed to Xiaoxin Zhang or Martin Brandt.

Peer review information *Nature Cities* thanks Kangning Huang and the other, anonymous, reviewer(s) for their contribution to the peer review of this work.

https://doi.org/10.1038/s44284-025-00227-9

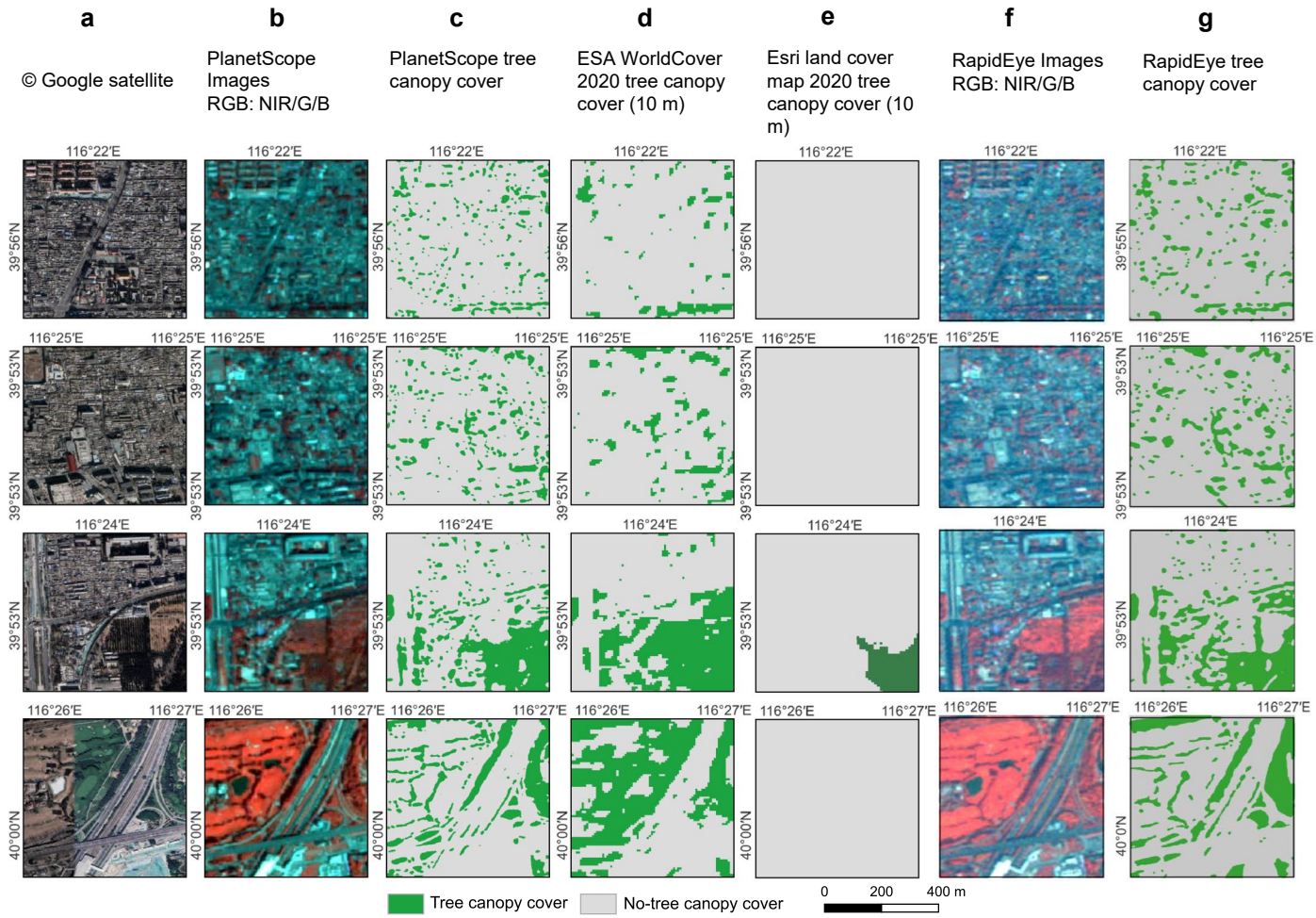

Extended Data Fig. 1 | Comparison of PlanetScope tree canopy mapping with other products. a, Google Earth satellite images (Google, 2023 Maxar Technologies). **b**, PlanetScope Image 2019 (RGB: NIR/G/B). Credit: Planet Labs PBC. **c**, PlanetScope tree canopy mapping 2019. **d**, Tree canopy from the ESA 2020 Land cover map[32]. **e**, Tree canopy based on the Esri land cover map 2020[59]. **f**, RapidEye image 2019 (RGB: NIR/G/B). Credit: Planet Labs PBC. **g**, RapidEye tree canopy cover in 2019.

https://doi.org/10.1038/s44284-025-00227-9

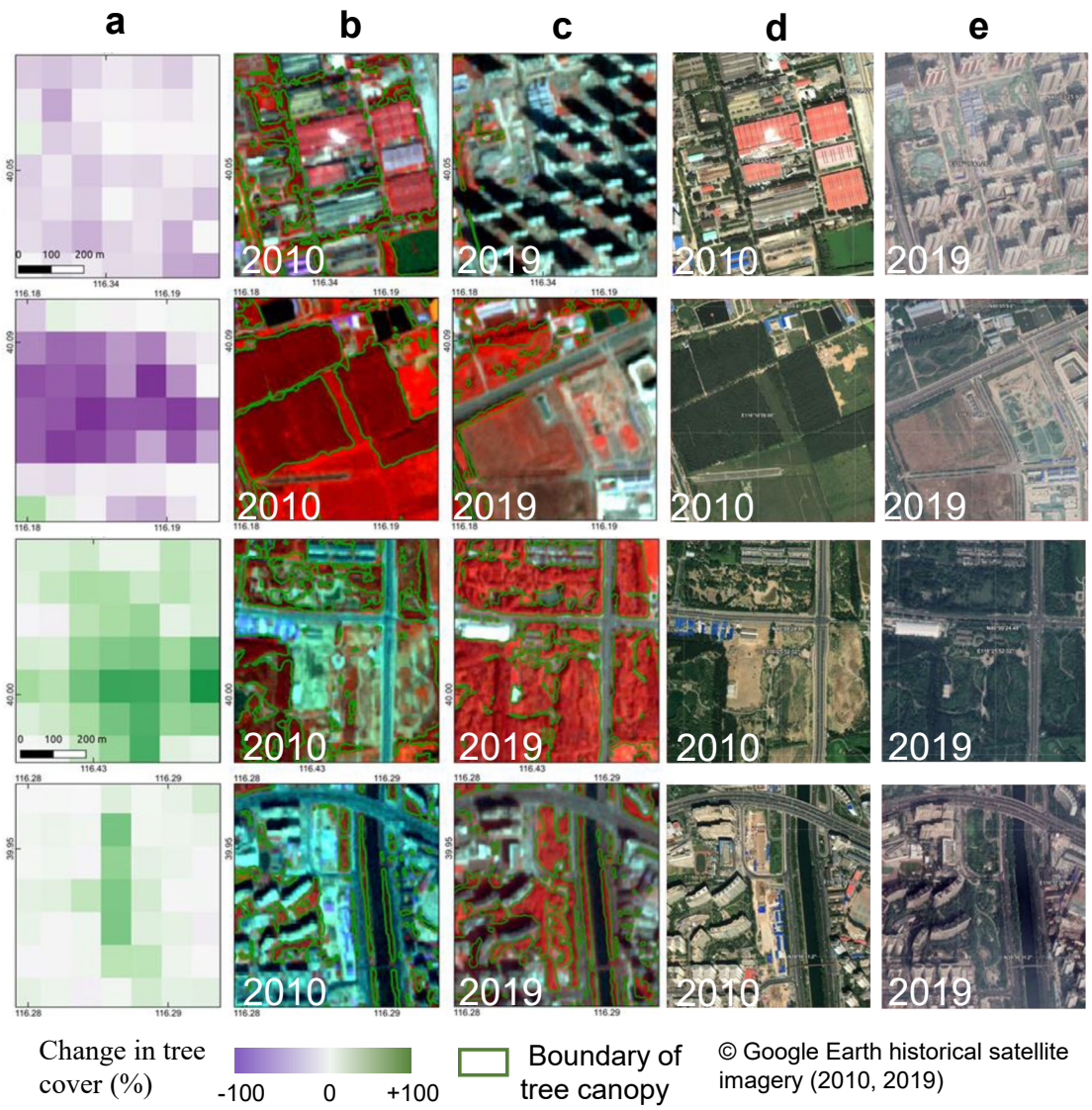

Extended Data Fig. 2 | Examples showing changes in tree canopy cover from 2010 to 2019. a, Change in tree cover in 1 ha grids (2010–2019). **b**, The prediction of tree canopy cover is based on RapidEye imagery in 2010. **c**, The prediction of tree canopy cover is based on PlanetScope imagery in 2019. **d**, Google Earth historical imagery in 2010 (Google, 2024 Maxar Technologies). **e**, Google Earth historical imagery in 2019 (Google, 2024 Maxar Technologies).

https://doi.org/10.1038/s44284-025-00227-9

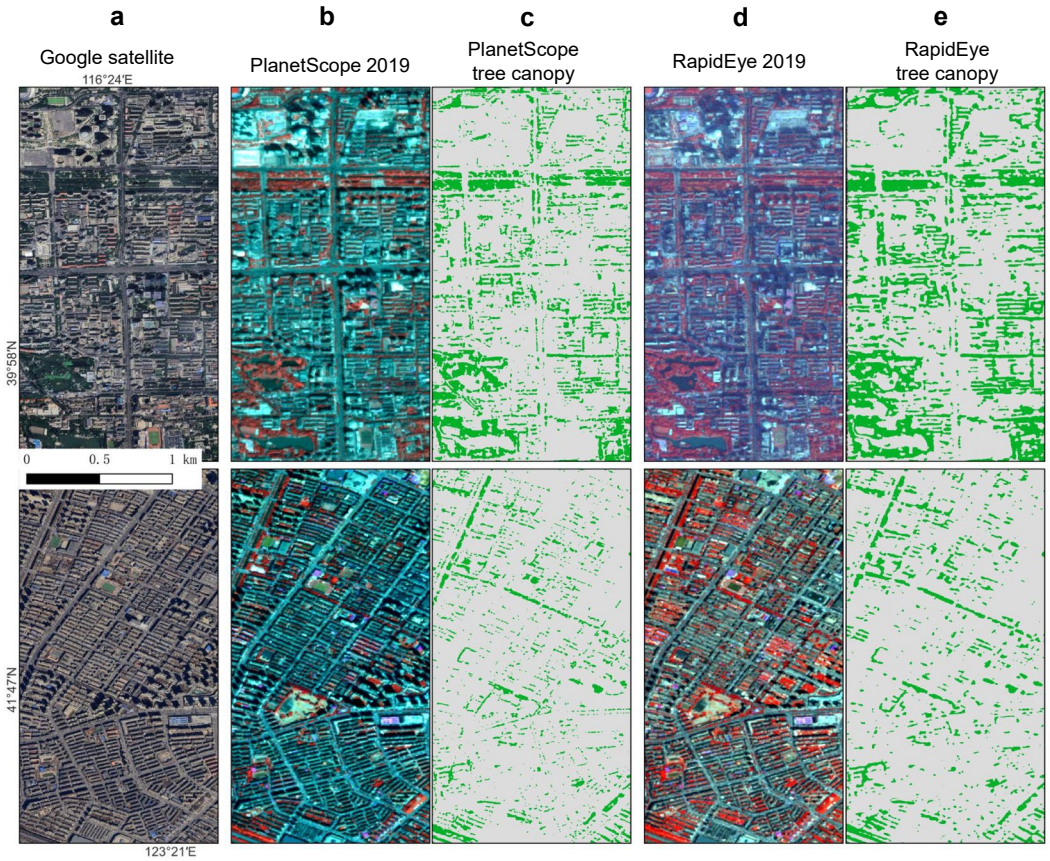

Extended Data Fig. 3 | Comparison of PlanetScope and RapidEye in 2019. a, Google Earth satellite images (Google, 2024 Maxar Technologies). **b**, PlanetScope Image 2019 (RGB: NIR/G/B). **c**, PlanetScope tree canopy cover in 2019. **d**, RapidEye image 2019 (RGB: NIR/G/B). **e**, RapidEye tree canopy cover in 2019.

https://doi.org/10.1038/s44284-025-00227-9

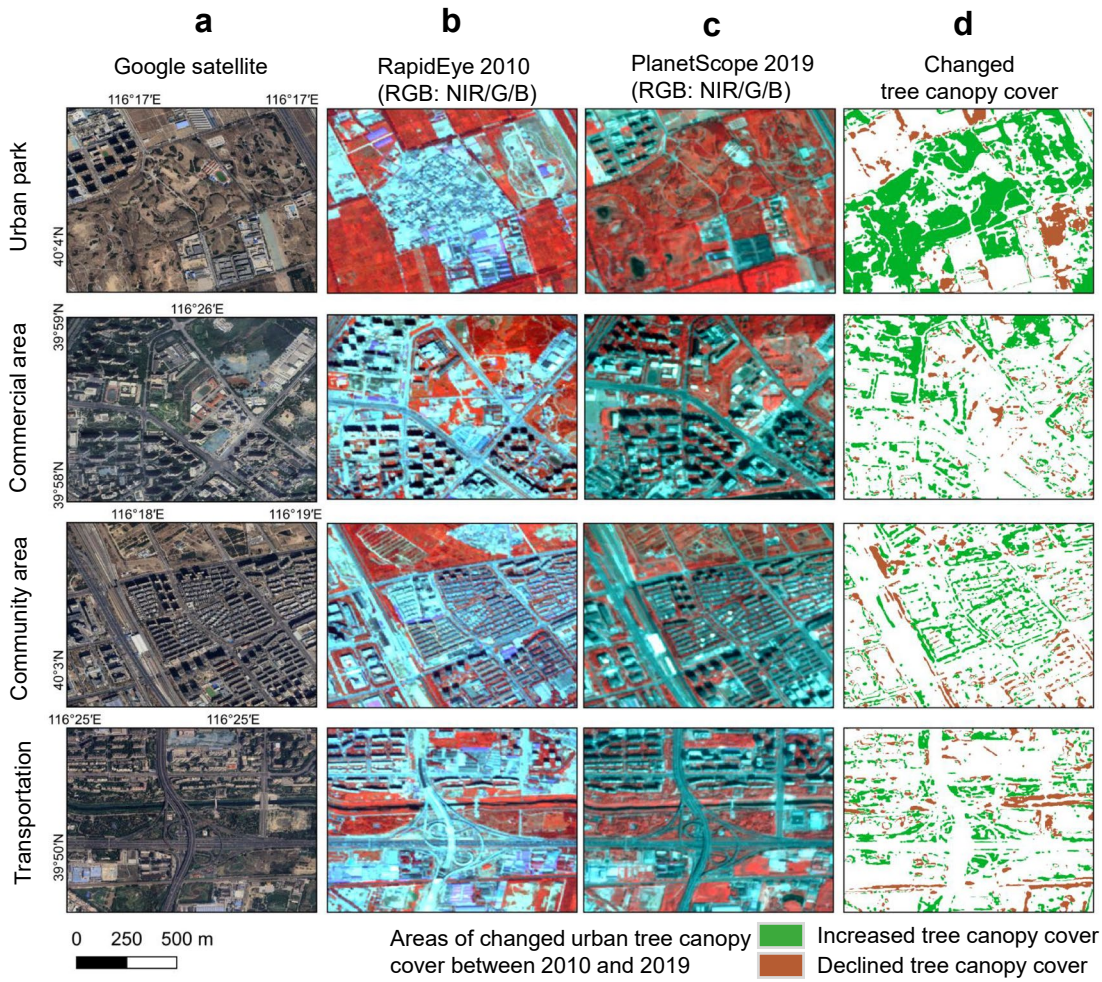

Extended Data Fig. 4 | Examples of urban greening in various urban land use types. a, Google Earth satellite images (Google, 2024 Maxar Technologies). **b**, RapidEye Image 2010 (RGB: NIR/G/B). **c**, RapidEye image 2019 (RGB: NIR/G/B). **d**, Areas of increasing and decreasing urban tree canopy cover between 2010 and 2019, with unchanged canopy areas excluded. Credit: **a**, Google Earth; **b**,**c**: Planet Labs PBC.

https://doi.org/10.1038/s44284-025-00227-9

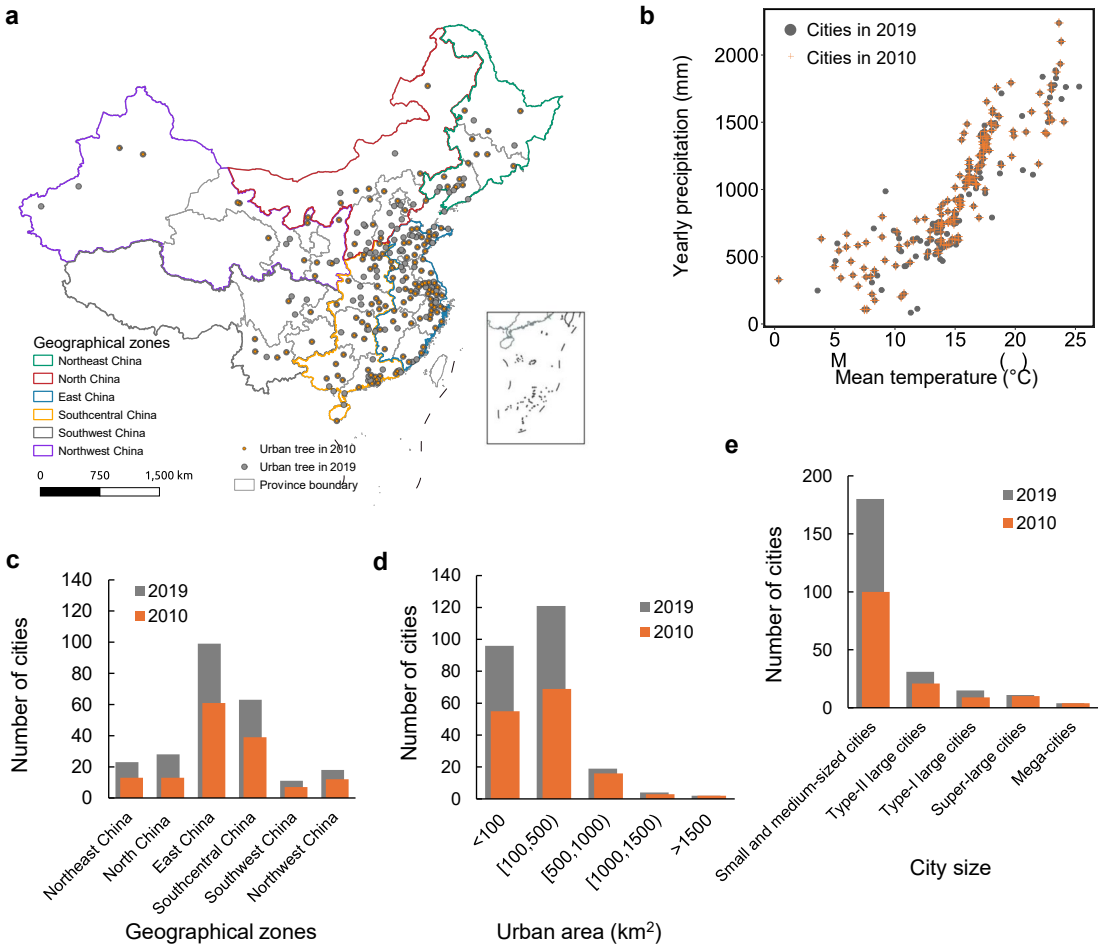

Extended Data Fig. 5 | Cities studied in 2010 (n = 144) and 2019 (n = 242). a, Spatial distribution of cities studied in 2010 and 2019. **b**, Mean temperature and annual precipitation of cities analyzed. **c**, Number of cities in the different geographical zones. **d**, Urban areas of the analyzed cities. **e**, Cities grouped by their population size (see Methods).

https://doi.org/10.1038/s44284-025-00227-9

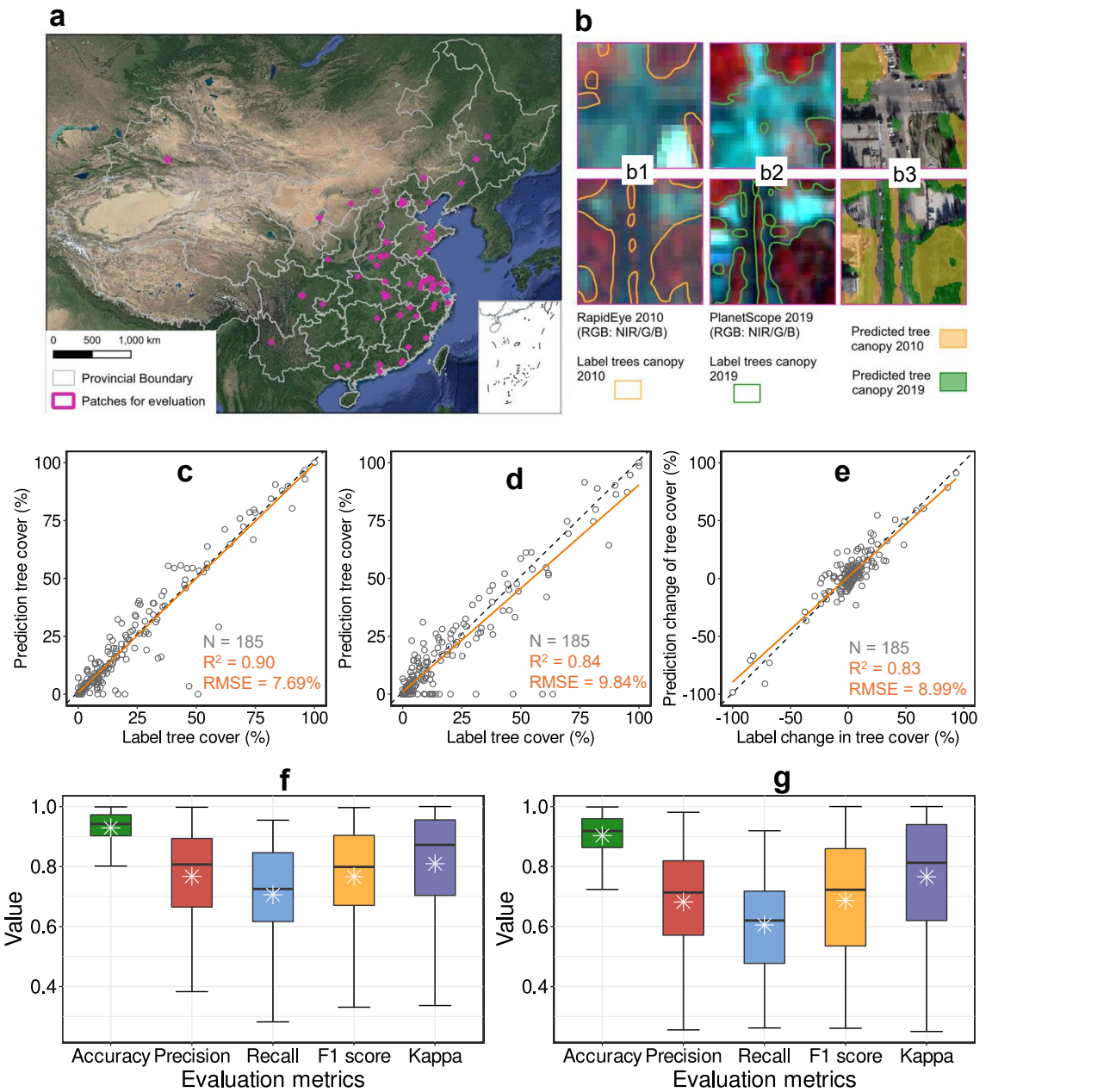

Extended Data Fig. 6 | Comparison between manually labeled areas from the test dataset and the corresponding predictions for 185 patches (the size of each patch is 1 ha). a, Location of patches for evaluation. Map data retrieved from Google, 2023 Maxar Technologies. **b**, Examples of patches with labeled tree canopy cover for 2010 (b1) and 2019 (b2) and prediction (b3). **c**, Comparison between predictions and manual labeling for PlanetScope 2019 tree canopy cover. **d**, Comparison between predictions and manual labeling for RapidEye 2010 tree canopy cover. **e**, Comparison of tree canopy cover changes from 2010 to 2019 between model predictions and manual labeling. **f**, Statistical evaluation metrics for the PlanetScope 2019 tree canopy cover mapping (※: mean value; −: median value). **g**, Statistical evaluation metrics for the RapidEye 2010 tree canopy cover mapping (※: mean value; −: median value). Basemap in **a** is from Google Maps Google Earth Satellite Imagery from 2023 (Imagery 2023, Maxar Technologies). In the box plots the lower and upper box limits are the 25th and 75th percentiles, the central line is the median, and the upper (lower) whiskers extend to 1.5 (−1.5) times the interquartile range.

https://doi.org/10.1038/s44284-025-00227-9

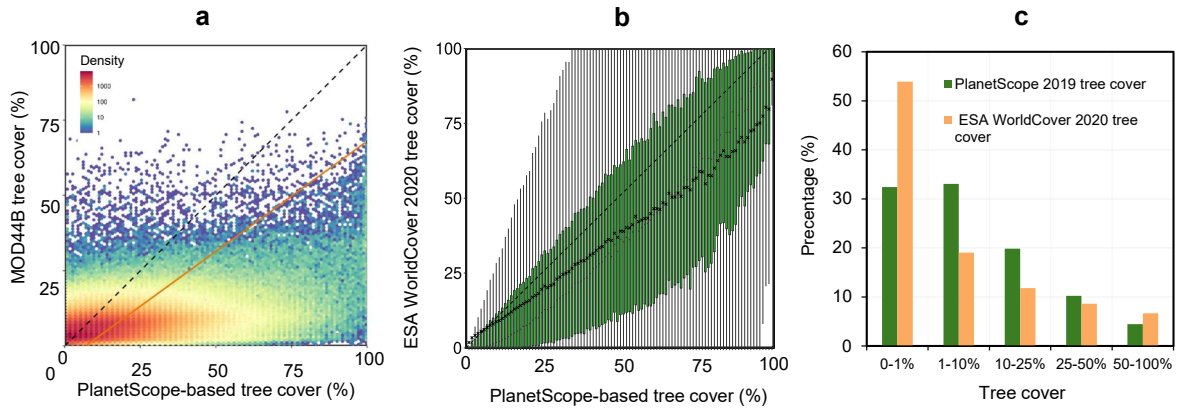

Extended Data Fig. 7 | Comparison of tree cover predictions from PlanetScope and other tree cover products in urban areas. a, Density plot for the PlanetScope-based 2019 tree cover and MOD44B 2019 tree cover. **b**, Box plot for the PlanetScope-based 2019 tree cover and ESA WorldCover 2020[32] tree cover (×: mean value; –: median value). **c**, Histogram of PlanetScope 2019 tree cover and ESA WorldCover 2020[32] tree cover in urban areas. In the box plots the lower and upper box limits are the 25th and 75th percentiles, the central line is the median, and the upper (lower) whiskers extend to 1.5 (−1.5) times the interquartile range.

https://doi.org/10.1038/s44284-025-00227-9

Extended Data Table 1 | Mean tree cover by land cover class. Land cover classes are derived from the ESA WorldCover 2020 map[32]

Land cover type (ESA WorldCover 2020)	Total area (km^2)	PlanetScope tree cover (%)
Tree Cover	65291.74	48.26
Shrubland	806.22	23.02
Grassland	11301.15	14.24
Cropland	74083.89	17.59
Built-up	401606.23	6.79
Bare/sparse vegetation	85634.48	6.41
Permanent water bodies	9461.42	5.27
Herbaceous wetland	161.62	12.46

nature portfolio

Corresponding author(s): Xiaoxin Zhang

Last updated by author(s): Jan 20, 2025

Reporting Summary

Nature Portfolio wishes to improve the reproducibility of the work that we publish. This form provides structure for consistency and transparency in reporting. For further information on Nature Portfolio policies, see our Editorial Policies and the Editorial Policy Checklist.

Statistics

For all statistical analyses, confirm that the following items are present in the figure legend, table legend, main text, or Methods section.

n/a	Confirmed
☐	☒ The exact sample size (*n*) for each experimental group/condition, given as a discrete number and unit of measurement
☒	☐ A statement on whether measurements were taken from distinct samples or whether the same sample was measured repeatedly
☐	☒ The statistical test(s) used AND whether they are one- or two-sided *Only common tests should be described solely by name; describe more complex techniques in the Methods section.*
☐	☒ A description of all covariates tested
☐	☒ A description of any assumptions or corrections, such as tests of normality and adjustment for multiple comparisons
☐	☒ A full description of the statistical parameters including central tendency (e.g. means) or other basic estimates (e.g. regression coefficient) AND variation (e.g. standard deviation) or associated estimates of uncertainty (e.g. confidence intervals)
☐	☒ For null hypothesis testing, the test statistic (e.g. *F*, *t*, *r*) with confidence intervals, effect sizes, degrees of freedom and *P* value noted *Give P values as exact values whenever suitable.*
☒	☐ For Bayesian analysis, information on the choice of priors and Markov chain Monte Carlo settings
☒	☐ For hierarchical and complex designs, identification of the appropriate level for tests and full reporting of outcomes
☒	☐ Estimates of effect sizes (e.g. Cohen's *d*, Pearson's *r*), indicating how they were calculated

Our web collection on statistics for biologists contains articles on many of the points above.

Software and code

Policy information about availability of computer code

Data collection	We used open source python (3.8.6) to collect dataset. the code is available Code for preparation of imagery from PlanetScope raw scenes has been deposited in the Zenodo database and is available at https://doi.org/10.5281/zenodo.7764359
Data analysis	We used open-source Python (version 3.8.6) to perform the analysis. The code for the tree canopy detection framework based on U-Net is publicly available at https://doi.org/10.5281/zenodo.3978185.

For manuscripts utilizing custom algorithms or software that are central to the research but not yet described in published literature, software must be made available to editors and reviewers. We strongly encourage code deposition in a community repository (e.g. GitHub). See the Nature Portfolio guidelines for submitting code & software for further information.

Data

Policy information about availability of data

All manuscripts must include a data availability statement. This statement should provide the following information, where applicable:

- Accession codes, unique identifiers, or web links for publicly available datasets
- A description of any restrictions on data availability
- For clinical datasets or third party data, please ensure that the statement adheres to our policy

The high-resolution tree canopy and changes in tree cover can be visualized at https://ee-xzrscph.projects.earthengine.app/view/china-urban-tree-change. PlanetScope imagery and RapidEye imagery in urban areas over China is available from Planet Labs (https://www.planet.com/products/) upon acquiring a license

agreement. GlobeLand30 land cover dataset (2010, 2020) is available at http://www.globallandcover.com/home_en.html. The ESA WorldCover 2020 land cover map can be downloaded at https://worldcover2020.esa.int/. Annual maps for the global artificial impervious areas (GAIA) dataset can be downloaded from http://data.ess.tsinghua.edu.cn. The essential urban land use categories map in China (EULUC-China) is available at http://data.ess.tsinghua.edu.cn/. Population density data from WorldPop in 2019 can be downloaded at https://www.worldpop.org. The administrative boundaries in China are accessible from the national catalog service for geographic information (https://www.ngcc.cn/).

Research involving human participants, their data, or biological material

Policy information about studies with human participants or human data. See also policy information about sex, gender (identity/presentation), and sexual orientation and race, ethnicity and racism.

Reporting on sex and gender	NA
Reporting on race, ethnicity, or other socially relevant groupings	NA
Population characteristics	NA
Recruitment	NA
Ethics oversight	NA

Note that full information on the approval of the study protocol must also be provided in the manuscript.

Field-specific reporting

Please select the one below that is the best fit for your research. If you are not sure, read the appropriate sections before making your selection.

☐ Life sciences ☐ Behavioural & social sciences ☒ Ecological, evolutionary & environmental sciences

For a reference copy of the document with all sections, see nature.com/documents/nr-reporting-summary-flat.pdf

Ecological, evolutionary & environmental sciences study design

All studies must disclose on these points even when the disclosure is negative.

Study description	We used PlanetScope satellite data for 2019 and RapidEye imagery for 2010 to map urban tree cover and study the dynamics of trees between 2010 and 2019 in urban areas across China.
Research sample	The data used for this study consisted of 3-meter, 4-band satellite imagery from PlanetScope, and 5-meter, 5-band satellite imagery from RapidEye. The study area comprises China's urban areas, defined by a land cover map. The high-resolution satellite images were obtained from Planet Labs via their API, with raw scenes downloaded through the Planet API and then merged into 1x1 degree composite mosaics. The satellite imagery for 2010 and 2019 was then clipped to match the urban areas.
Sampling strategy	Urban areas larger than 50 km² and available within cloud-free PlanetScope and RapidEye coverage are included.
Data collection	High-resolution imagery from two satellites was collected through the Planet API by Florian Reiner, Martin Brandt, and Xiaoxin Zhang.
Timing and spatial scale	The date range for each mosaic is specific to the phenology of the urban areas cover 245 cities in China for 2019 and 145 cities for 2010.
Data exclusions	Among all available PlanetScope and RapidEye images, scenes were filtered first by date range using the phenology-determined temporal window, and then by quality using API filters based on factors such as percent cloud cover, haze, and visual confidence. From these selected scenes, only a subset was used to create a gap-less mosaic. Scene footprints were clipped prior to downloading to minimize redundant data retrieval.
Reproducibility	With the deep learning framework used, predication of trees canopy cover is deterministic, i.e.. predicting the same image several times will always give the same results.
Randomization	NA
Blinding	NA

Did the study involve field work? ☐ Yes ☒ No

Reporting for specific materials, systems and methods

We require information from authors about some types of materials, experimental systems and methods used in many studies. Here, indicate whether each material, system or method listed is relevant to your study. If you are not sure if a list item applies to your research, read the appropriate section before selecting a response.

Materials & experimental systems

n/a	Involved in the study
☒	☐ Antibodies
☒	☐ Eukaryotic cell lines
☒	☐ Palaeontology and archaeology
☒	☐ Animals and other organisms
☒	☐ Clinical data
☒	☐ Dual use research of concern
☒	☐ Plants

Methods

n/a	Involved in the study
☒	☐ ChIP-seq
☒	☐ Flow cytometry
☒	☐ MRI-based neuroimaging

Plants

Seed stocks	NA
Novel plant genotypes	NA
Authentication	NA